# Data-driven "cross-component" design and optimization of γ′-strengthened Co-based superalloys

*Song Lu, Min Zou, Xiaorui Zhang, Stoichko Antonov, Wendao Li, Longfei Li*, Qiang Feng**

S. Lu, M. Zou, X. Zhang, W. Li, L. Li, Q. Feng
Beijing Advanced Innovation Center for Materials Genome Engineering, State Key Laboratory for Advanced Metals and Materials, University of Science and Technology Beijing, Beijing 100083, China
Corresponding authors: *L. Li (lilf@skl.ustb.edu.cn) and Q. Feng (qfeng@skl.ustb.edu.cn)*

W. Li
School of Materials Science and Engineering, Xiangtan University, Xiangtan 411105, China

S. Antonov
Department of Microstructure Physics and Alloy Design, Max-Planck-Institut für Eisenforschung GmbH, 40237 Düsseldorf, Germany

**Keywords:** Co-based superalloy; machine-learning; diffusion-multiple; "cross-component" prediction; alloy design

**Abstract:**

The design of complex multi-component superalloys has always been challenging due to the interaction of multiple elements and stringent requirements for various properties. In this study, an integrated approach to designing the high-component (>7) γ′-strengthened Co-based superalloys with well-balanced properties is developed by combining the diffusion-multiples and machine-learning models. A "cross-component" prediction is achieved by the machine-learning models, where two types of novenary superalloys are screened out for aero-engine and industrial gas turbine blades, respectively, based on the experimental database mainly consisting of 6-7 elements. The method is verified to be effective or slightly more favorable than the Calculation of Phase Diagram (CALPHAD) in predicting the γ′ solvus temperature ($T_{\gamma'}$) and phase constituent of the high-

This article has been accepted for publication and undergone full peer review but has not been through the copyediting, typesetting, pagination and proofreading process, which may lead to differences between this version and the Version of Record. Please cite this article as doi: 10.1002/adem.202201257.

This article is protected by copyright. All rights reserved

Accepted Article

15272648, 2023, 0, Downloaded from https://onlinelibrary.wiley.com. By MPI 337 Iron Research - on 02. Februar 2023. Re-use and distribution is strictly not permitted, except for Open Access articles

component alloys when reasonable data of low-component alloys is just provided. Furthermore, the oxidation resistance and hardness of polycrystal superalloys as well as the compressive strength of single crystal superalloys are tested. Finally, some factors affecting the accuracy of "cross-component" prediction are discussed. Expanding the compositional range and supplementing the critical interaction data of multiple elements in the database are beneficial for improving the accuracy of the "cross-component" prediction.

## 1. Introduction

The discovery of ordered γ′ precipitates in the system of Co-Al-W-based alloys paves a new pathway for the development of high-temperature superalloys applied at high temperatures.[1][2] Compared to the widely used Ni-based superalloys, the potential for higher temperature capability is expected with Co-based superalloys due to the higher melting temperature of the major matrix component, Co.[3][4] This is very attractive for hot-end components in advanced aero-engines to further improve the fuel efficiency and mechanical properties. In addition, Co-based superalloys usually have a higher sulfide melting temperature than Ni-based superalloys, which is beneficial for the long-term service in an environment containing sulfur, such as industrial gas turbines.[4] However, due to the complexity of the actual service environment, commercial superalloys need to fulfill a variety of physical and chemical properties simultaneously, such as creep, fatigue, oxidation, corrosion and density, which is done by tailoring the alloy composition typically comprising of more than 9 components.[5]

Until now, the research of γ′-strengthened Co-based superalloys has gradually evolved from exploring alloying principles, considering individual or multiple elements,[6]–[8] to the optimization of different properties in an alloy with complex components (≥ 7).[9]–[11] Many researchers have demonstrated that Ni addition can significantly expand the γ+γ′ phase region,[12][13] which contributes to the tailoring of the microstructure by the addition of other refractory elements. Thus, a series of CoNi-based superalloys have been developed in recent years. Ta, Ti and Nb improve the γ′ solvus temperature ($T_{\gamma'}$) and the temperature capability,[14]–[16] while they also promote the precipitation of TCP phases, which are harmful to mechanical properties.[17][18] Cr is beneficial for improving the oxidation and corrosion resistance, but it reduces the $T_{\gamma'}$ and area fraction of γ′ precipitates ($A_{\gamma'}$).[19][20] Mo, W and Re provide good solid solution strengthening effects in Ni-based superalloys with a negative misfit ($a_{\gamma'} < a_{\gamma}$). In contrast, Mo lowers the misfit of γ′-strengthened Co-based superalloys, which generally exhibit a positive misfit ($a_{\gamma'} > a_{\gamma}$), by increasing the lattice constant of the γ matrix. This normally results in a transition of the γ′ precipitate morphology from cuboidal to spherical,[21] which is beneficial for the microstructural stability during the long-term service process. W is the γ′-forming element in γ′-strengthened Co-based superalloys,[22] and its solution effect is lower than that

This article is protected by copyright. All rights reserved

Accepted Article

15272648, 2023, 0, Downloaded from https://onlinelibrary.wiley.com. By MPI 337 Iron Research - on 02. Februar 2023. Re-use and distribution is strictly not permitted, except for Open Access articles

in Ni-based superalloys. Moreover, the addition of W will greatly increase the density. Although Re can significantly improve the creep resistance of Ni-based superalloys by strongly segregating to the γ matrix, lowering the effective diffusion coefficients and leading to a large lattice distortion, no obvious improvement of creep property is detected in the γ′-strengthened Co-based superalloys containing Re.[23] Thus, it is essential to understand the synergetic effects of multiple elements when making compositional optimization of γ′-strengthened Co-based superalloys.

In the early days of CoNi-based superalloy research, conventional methods were used to prepare a series of individual alloys and further screened them by their $T_{\gamma'}$, phase constituents, density, oxidation and so on.[10][21][24] Due to the limitation of experimental methods and databases, it was difficult to realize a synergistic consideration and optimization of multiple physical and chemical properties. To accelerate the design process, calculation methods like density functional theory (DFT) and thermodynamic calculation were applied based on the materials knowledge. Even so, the DFT calculation of superalloys within a complex system would consume extended time and be costly. Thermodynamic calculation can efficiently navigate the relationship among the complex compositions and some physical properties, such as the $A_{\gamma'}$, $T_{\gamma'}$ and phase constituents. But the accuracy of the Calculation of Phase Diagram (CALPHAD) is strongly affected by the accuracy and size of the thermodynamic database. Until now, significant amount of experimental or simulative works have been performed to improve the effectiveness of the thermodynamic database, especially for the high-component alloys. Even so, the CALPHAD method was ineffective at predicting phase equilibria behavior when Cr is introduced to Co-Ni-Al-W, as reported by Lass [25]. Similar results were also reported in the high-component γ′-strengthened Co-based superalloys containing W, Ta, Mo or Nb.[11][25]–[27] Thus, it is important to develop a novel approach for efficiently predicting the complex system's properties.

Machine-learning has been recently introduced into the design of γ′-strengthened Co-based superalloys due to the superiority and high efficiency in processing a large amount of multi-dimensional data.[11][21][27][28] One or more properties have been simultaneously considered in these studies. Moreover, all of these researches show that the prediction accuracy strongly depends on the quality and quantity of the database, although multiple algorithms were employed and carefully optimized to build the machine-learning models. However, it is difficult and costly to produce a large amount of high-quality data using traditional experimental approaches. Thus, Liu et al.[11] integrated the composition-microstructure data calculated by the CALPHAD into the machine-learning model, and predicted the behavior of some septenary γ′-strengthened Co-based superalloys. However, as mentioned the low accuracy of thermodynamic databases, especially around phase boundaries, is still a hurdle and the deleterious phases precipitated in predicted alloys. Additionally, experimental

This article is protected by copyright. All rights reserved

Accepted Article

15272648, 2023, 0, Downloaded from https://onlinelibrary.wiley.com. By MPI 337 Iron Research - on 02. Februar 2023. Re-use and distribution is strictly not permitted, except for Open Access articles

databases were also built to predict the Co-Ti-V-X[29] or CoNi-based alloy systems[27] based on the individual traditional experimental approaches and published results. This has been verified to be available for the quick search for the γ′-strengthened Co-based superalloys with high $T_{\gamma'}$. However, large deviations were exhibited in the machine-learning predictions of phase constituents and $A_{\gamma'}$.[11][27][30] All the methods mentioned above cannot compensate for the insufficient high-quality data. Thus, the prediction is normally carried out within a selected database to find a local maximum or minimum.[31] It is difficult to extrapolate outside the database, let alone perform the "cross-component" prediction, wherein the prediction has higher components than the alloys in the database. In fact, the "black box" in machine-learning models also involves calculations, which may not be understandable, of the synergetic effects of multiple elements. As such, it is theoretically possible for the machine-learning model to make a "cross-component" prediction, when the database is accurate enough and the correct algorithms are selected and trained properly.

Multicomponent diffusion-multiple is a high-throughput experimental method, which can quickly obtain a large amount of quantitative experimental data in a wide range of compositions.[32][33] Moreover, compared to the underpopulated CALPHAD databases, the diffusion multiples have an obvious advantage in determining the phase boundaries in γ′-strengthened Co-based superalloys. The high accuracy of experimental data around the phase boundaries can also be used to supplement the CALPHAD databases, as reported in our previous works.[26][34] Therefore, it is expected to improve the accuracy of prediction within the database and allow for "cross-component" predictions by integrating the diffusion-multiple with the machine-learning model.

In this study, a large database on the relationship between the compositions and microstructures was established by two multicomponent diffusion-multiples. Additionally, some data, including the microstructure and $T_{\gamma'}$, was obtained from individual experiments in our previous works and related literature. Subsequently, a machine-learning framework was constructed to perform "cross-component" predictions of γ′-strengthened Co-based superalloys containing up to 9 elements, based on domain knowledge-driven empirical design criteria for the aero-engines and industrial gas turbines. Polycrystal and single crystal alloys were produced to verify some critical physical and chemical properties. Optimization strategies for the "diffusion-multiple + machine-learning" method are further proposed based on the experimental results of the prediction superalloys. This work will be significant for accelerating the development of alloys with complex components.

## 2. Results and Discussions

### 2.1. Workflow of Machine-Learning Strategy

This article is protected by copyright. All rights reserved

Accepted Article

15272648, 2023, 0, Downloaded from https://onlinelibrary.wiley.com. By MPI 337 Iron Research - on 02. Februar 2023. Re-use and distribution is strictly not permitted, except for Open Access articles

The upper temperature capability strongly depends on the $T_{\gamma'}$, i.e., γ′ strengthening is provided below this temperature. In addition, the microstructural stability (phase constituent) and $A_{\gamma'}$ at the service temperature are the critical parameters affecting the mechanical performance, viz. tensile/compressive, creep and fatigue properties. Therefore, the above three fundamental physical properties/parameters are mainly optimized in this study.

**Figure 1** shows the workflow of multi-performance optimization for γ′-strengthened Co-based superalloys by integrating experimental data and machine-learning models. First, a large experimental database consisting of the relationship among the alloy composition with the phase constituents, $T_{\gamma'}$ and $A_{\gamma'}$ was established. The data for the phase constituent and $A_{\gamma'}$ mainly comes from the diffusion-multiples (data set), individual experimental alloys (single data) of our group and published literature. In contrast, the data of $T_{\gamma'}$ was mainly obtained through individual experiments from our previous works and other published results. It should be noted that all data in the database comes from γ′-strengthened Co-based superalloys with 8 or less components, and most of them consist of 6~7 elements. This will be further detailed in the following sections.

A classification model was applied to predict the output values of phase constituent: "0" for γ single phase, "1" for γ/γ′ two-phase microstructure, and "2" denoting the existence of detrimental phases. A regression model was used to predict a numeric outcome ($T_{\gamma'}$ and $A_{\gamma'}$) of the input alloy composition. After that, several widely used machine-learning algorithms were further screened out by the exhaustive method to determine the optimal algorithm for the investigated composition-physical properties (phase constituents, $T_{\gamma'}$ and $A_{\gamma'}$) relationships. Random Forest (RF), XGBoost (eXtreme Gradient Boosting, also known as GBDT), Deep Neural Network (DNN), K-Nearest Neighbor (KNN) and Logistic Regression (LR) algorithms were employed to build the phase constituent classification model, and the validity was evaluated by the value of Macro-$F_1$.[35] Linear regressions (Lin), RF, GBDT, DNN and Support Vector Regression (SVR) with a radial basis function kernel were applied to build the $T_{\gamma'}$ and the $A_{\gamma'}$ regression models, and the validity was evaluated by the value of the root-mean-square error (RMSE) and the explained variance ($R^2$).

$$\mathrm{RMSE}=\sqrt{\frac{1}{n}\sum_{i=1}^{n}(Y_{act}-Y_{pre})^2} \qquad (1)$$

$$R^2=1-\frac{\sum_{i=1}^{n}(Y_{act}-Y_{pre})^2}{\sum_{i=1}^{n}(Y_{act}-Y_{ave})^2} \qquad (2)$$

where $Y_{act}$ is the true value, $Y_{pre}$ is the predicted value, $Y_{ave}$ is the average of $Y_{act}$, and n is the number of the predicted data in the dataset. The responses of Macro-$F_1$ and $R^2$ range from 0 to 1, where the better the model performance, the closer the value is to 1, and the RMSE value is smaller. Models were adjusted until the optimal model performance was obtained.[11][21] Then, the models were

This article is protected by copyright. All rights reserved

Accepted Article

15272648, 2023, 0, Downloaded from https://onlinelibrary.wiley.com. By MPI 337 Iron Research - on 02. Februar 2023. Re-use and distribution is strictly not permitted, except for Open Access articles

employed to predict the phase constituent, $T_{\gamma'}$ and $A_{\gamma'}$ after the elements (up to nine) of γ′-strengthened Co-based superalloys were input. Finally, several objective alloy compositions were screened out based on the design criteria for different types of superalloys, and the reliability of the model was evaluated by systematic experiment investigations.

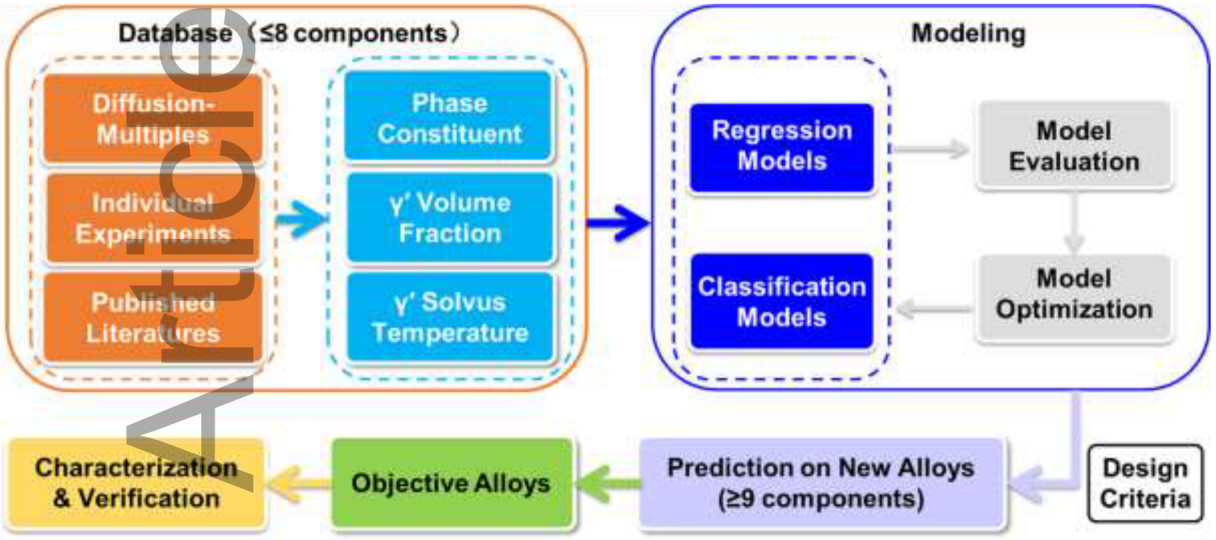


**Figure 1.** Workflow of multi-performance optimization for γ′-strengthened Co-based superalloys by integrating experimental data and machine-learning models.

2.1.1. Diffusion Multiple and Design Criteria

**Figure 2** exhibits the schematic of two multicomponent diffusion-multiples and the quantitative relationship between compositions and microstructures. The first diffusion-multiple shown in Figure 2(a) was used for the first-round alloy screening based on the microstructure. The base alloy1 was determined by our previous works on the single crystal Co-Al-W-based superalloy (Co-7Al-8W-4Ti-1Ta (at. %)), which has a comparable creep resistance with first-generation Ni-based single crystal superalloys.[36][37] Subsequently, Ni was added to expand the γ+γ′ phase region. The Co-20Ni-7Al-8W-4Ti-1Ta (at. %) alloy was selected as the base alloy to further tailor other elements considering the microstructural stability (Ni, W), creep resistance (Ti, Ta, Mo, Nb), density (Al) and oxidation resistance (Cr). Of note is that the maximum number of components is 7 in this diffusion-multiple. Combined with the first diffusion-multiple, some individual tests were performed to further verify the microstructural stability and oxidation resistance of the screened alloys. Then, a single crystal superalloy (Co-30Ni-11Al-4W-4Ti-1Ta-5Cr (at. %)) was obtained with a good combination of density, creep and oxidation resistance.[38] To further optimize the microstructural stability and oxidation resistance, the individual effects of Al, Cr, Ti, Ta, Mo and Ni on base alloy2 (Co-30Ni-11Al-4W-2Ti-1Ta-5Cr (at. %)) were investigated with a second diffusion-multiple, and the maximum

This article is protected by copyright. All rights reserved

Accepted Article

15272648, 2023, 0, Downloaded from https://onlinelibrary.wiley.com. By MPI 337 Iron Research - on 02. Februar 2023. Re-use and distribution is strictly not permitted, except for Open Access articles

component is 8 (Figure 2(b)). Additionally, the interaction of two or three elements can be investigated by analyzing the diffusion-couples around the base alloy2, such as +2Ta-+2Mo and +10Ni-+2Ti. Figure 2(c) shows the typical microstructural evolution with the variation in the concentrations of Mo and Ta in the +2Mo-+2Ta diffusion couple after being annealed at 1000 °C for 1000 h. The cerulean and purple circles present the variation of Mo and Ta contents, respectively. The γ/γ′ microstructure was observed throughout the +2Mo-+2Ta diffusion couple. The morphology of γ′ precipitates changes from being more spherical to being more angular or cuboidal (viewed from other crystallographic directions, not shown here) with the increase of Ta (1→3 at. %) and simultaneous decrease of Mo (2→0 at. %). Meanwhile, the $A_{\gamma'}$ was measured to increase from the alloy +2Mo (~80%) to +2Ta (~87%) (Figure S1, Supporting Information). Accordingly, 81 datasets of the phase constituent and the $A_{\gamma'}$ associated with compositions were obtained from each diffusion couple. Thus, by integrating the two diffusion couples and references[21][39]–[45], 2275 datasets were provided for the phase constituent and $A_{\gamma'}$ models mentioned in Figure 1. For the $T_{\gamma'}$ model, 238 datasets were collected from references[11][13][25][39][40][46]–[53] and our individual experiments.

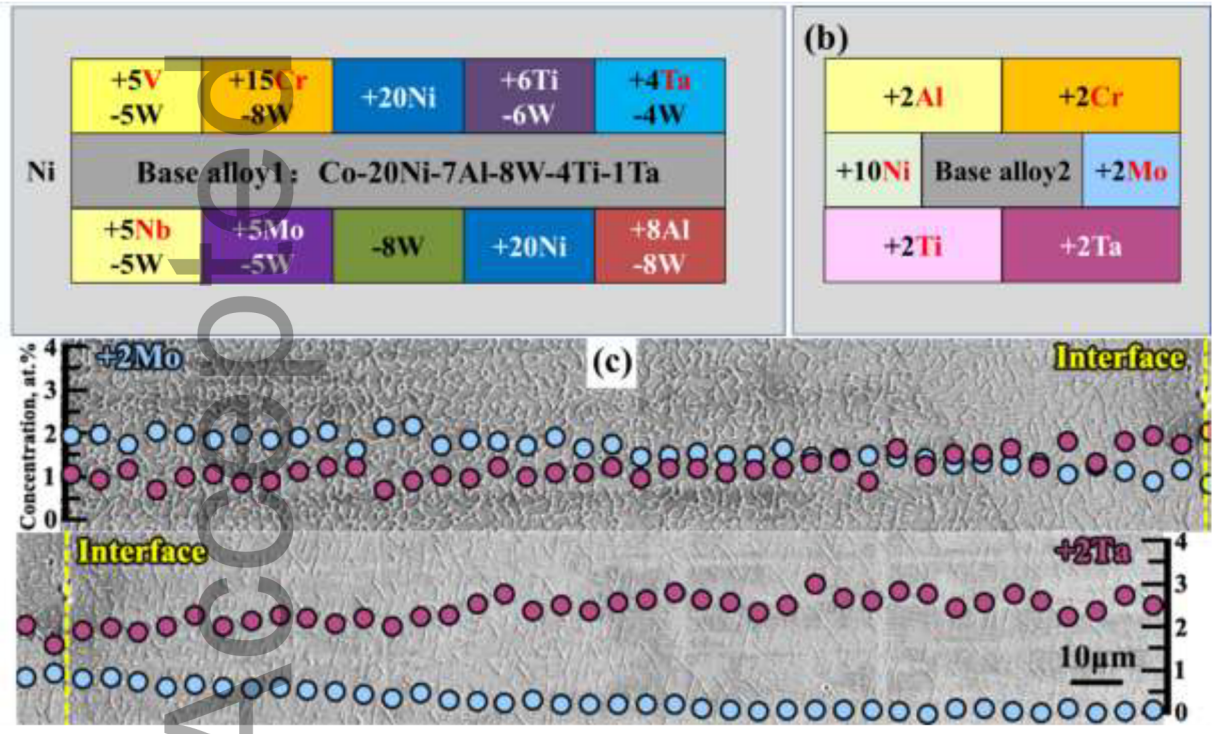


**Figure 2.** Schematic of two multicomponent diffusion-multiples and the quantitative relationship between compositions and microstructures. Diffusion-multiple used for the (a) first and (b) second rounds of the alloy screening. (c) Typical microstructural evolution with the variation of the

This article is protected by copyright. All rights reserved

15272648, 2023, 0, Downloaded from https://onlinelibrary.wiley.com. By MPI 337 Iron Research - on 02. Februar 2023. Re-use and distribution is strictly not permitted, except for Open Access articles

Accepted Article

concentrations of Mo and Ta in the +2Mo-+2Ta diffusion couple after being annealed at 1000 °C for 1000 h.

As mentioned in Figure 1, the final database was established by integrating the dataset from the diffusion-multiples (phase constituents, $A_{\gamma'}$) and independent data from individual experiments ($T_{\gamma'}$, phase constituents, $A_{\gamma'}$). Different machine-learning models were applied to the aforementioned three types of data. Moreover, the validity was evaluated and optimized by the value of Macro-F1 (phase constituent classification models), RMSE and $R^2$ ($T_{\gamma'}$ and $A_{\gamma'}$ regression models). Among the eight typical algorithms introduced in Figure 1, the GBDT algorithm had the best performance for predicting the phase constituents, $T_{\gamma'}$, and $A_{\gamma'}$ of the new γ′-strengthened Co-based superalloys with a number of components up to 9 (details of values Macro-F1, RMSE and $R^2$ for each model are shown in **Figure S2**).

Besides the $T_{\gamma'}$, phase constituent and $A_{\gamma'}$, additional properties like density and oxidation resistance need to be considered due to the requirements for different service environments. As such, combined with the domain knowledge and experience, two types of design criteria of superalloys were set for aero-engine and industrial gas turbine blades, respectively, as shown in **Table 1**. For the aero-engine, the superalloys generally work at a higher temperature (1000~1100 °C) than the industrial gas turbine (900~1000 °C). Thus, higher $T_{\gamma'}$ (≥1190 °C), good microstructural stability (γ+γ′) and $A_{\gamma'}$ (70~80%) at 1000 °C were preliminary set based on the existing experience.[54][55] The above three fundamental physical properties/parameters were predicted by the corresponding machine learning models. The design criteria for density and oxidation resistance were set as <8.8 g/cm$^3$, calculated by the empirical formula, and Al+Cr≥ 16 at. % based on our previous experience.[19][56] Similarly, the design criteria of $T_{\gamma'}$, phase constituent and $A_{\gamma'}$, density as well as oxidation resistance for the superalloys in industrial gas turbine blades[57]–[59] were also listed respectively in Table 1. Moreover, an additional criterion of high Cr content (≥12 at. %) was proposed to meet the requirement for the corrosion environment in industrial gas turbines.

According to the above criteria and microstructure results in the database, the search space of superalloys in the aero-engines, $Co_aNi_bAl_cW_dTi_eTa_fCr_gMo_hNb_i$ (at. %), was determined as follows: 26%≤b≤32%, 8%≤c≤13%, 1%≤d≤4%, 1%≤e≤4%, 1%≤f≤4%, 4%≤g≤8%, 0%≤h≤1.5%, 0%≤i≤1.5%, a>b, c+g≥16, and a+b+c+d+e+f+g+h+i=100%. A composition variation step of 1 at. % was set for c~g, 2 at. % for b, and 0.5 at. % for h~i, which results in a total of 81920 candidates containing up to 9 elements. In contrast, the search space of the industrial gas turbine superalloys is characterized by the lower and upper limits of Al and Cr content (6%≤Al≤11%, 12%≤Cr≤16%). The search space for other elements and composition variation step are the same as the aero-engine, which gives a total of 122880 candidates to be explored.

This article is protected by copyright. All rights reserved

Accepted Article

15272648, 2023, 0, Downloaded from https://onlinelibrary.wiley.com. By MPI 337 Iron Research - on 02. Februar 2023. Re-use and distribution is strictly not permitted, except for Open Access articles

**Table 1**. Two types of design criteria of superalloys set for the aero-engine and industrial gas turbine blades based on the existing experience, respectively.

| Property | Aero-engine | Industrial gas turbine | |
|---|---|---|---|
| γ′ solvus temperature (°C) | ≥1190 | ≥1100 | Machine learning |
| Phase constituent at 1000 °C | γ+γ′ | γ+γ′ | Machine learning |
| γ′ area fraction at 1000 °C | 70~80% | 60~70% | Machine learning |
| Density (g/cm$^3$) | <8.8 | <9 | Empirical |
| Oxidation (at. %) | Al+Cr≥16 | Al+Cr≥16, Cr≥12 | Empirical |

## 2.2. Experimental Verification

Based on the machine-learning models and design criteria, a total of 183 and 238 candidate alloys were screened out for the aero-engines and industrial gas turbines, respectively. To further guarantee microstructural stability, objective alloys with a higher $T_{\gamma'}$ and lower density were further screened with the Pareto frontier method. **Table 2** lists the nominal compositions of four novenary alloys, where alloys 9CoNi-A and 9CoNi-B were designed for the aero-engines, while alloys 9CoNi-C and 9CoNi-D for the industrial gas turbines.

**Table 2.** Nominal compositions of four novenary alloys designed for the aero-engines and industrial gas turbines, respectively (at. %).

| | Alloy | Co | Ni | Al | W | Ti | Ta | Cr | Mo | Nb |
|---|---|---|---|---|---|---|---|---|---|---|
| Aero-engine | 9CoNi-A | Bal. | 32 | 12 | 2 | 1 | 3 | 4 | 0.5 | 0.5 |
| | 9CoNi-B | Bal. | 32 | 10 | 2 | 2 | 3 | 7 | 0.5 | 0.5 |
| Industrial gas turbine | 9CoNi-C | Bal. | 32 | 7 | 3 | 3 | 1.5 | 14 | 0.5 | 0.5 |
| | 9CoNi-D | Bal. | 32 | 9 | 2 | 2 | 3 | 12 | 0.5 | 0.5 |

### 2.2.1. Microstructural Stability

**Figure 3** shows the scanning electron microscopy images of microstructures in the four novenary alloys after aging at different temperatures and hours. Both alloys 9CoNi-A and 9CoNi-B remain γ/γ′ microstructure after aging at 1000 °C/500 h, and no detrimental phases were observed, as shown in Figures 4(a) and (b), respectively. The morphology of γ′ precipitates was cuboidal with an equivalent diameter ($D_{\gamma'}$) of 877 ± 266 nm in alloy 9CoNi-A, while in alloy 9CoNi-B, it was transformed into rounded-edge rectangles through a coarsening and connecting process. Thus, the $D_{\gamma'}$ was not calculated due to the irregular shape of γ′ precipitates. The $A_{\gamma'}$ of alloy 9CoNi-A (73.8 ± 1.2%) is higher than that of alloy 9CoNi-B (53.5 ± 3.2%), which is lower than the value set by the design

This article is protected by copyright. All rights reserved

Accepted Article

15272648, 2023, 0, Downloaded from https://onlinelibrary.wiley.com. By MPI 337 Iron Research - on 02. Februar 2023. Re-use and distribution is strictly not permitted, except for Open Access articles

criterion (70~80%) for the aero-engines (Table 1). The industrial gas turbine alloys 9CoNi-C and 9CoNi-D keep typical the γ/γ′ microstructure after aging at 950 °C/600 h, and the corners of the γ′ precipitates are smooth. The $A_{\gamma'}$ of alloys 9CoNi-C and 9CoNi-D were measured to be 51.1 ± 0.5% and 57.4 ± 0.8%, respectively. No noticeable difference of $D_{\gamma'}$ was found between alloys 9CoNi-C (373 ± 86 nm) and 9CoNi-D (388 ± 80 nm).

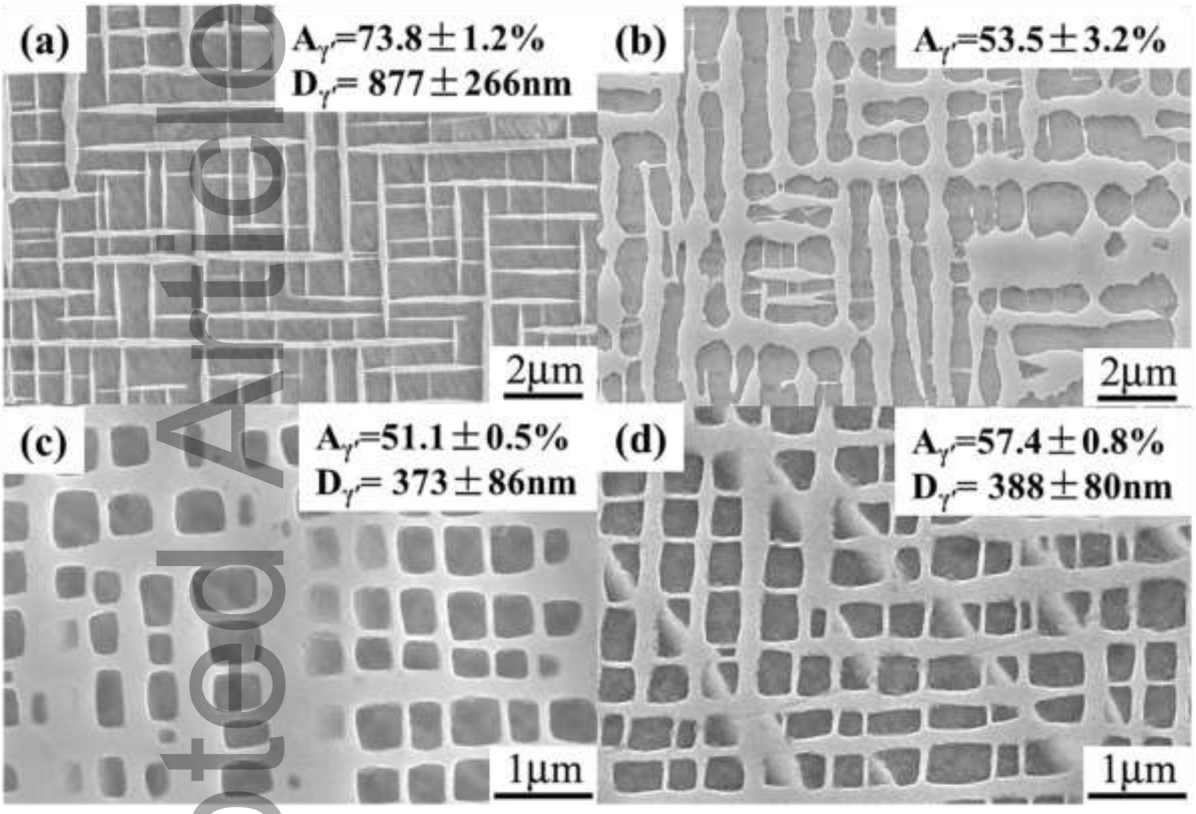


**Figure 3.** Scanning electron microscopy images of microstructures in four novenary alloys after aging at different temperatures and hours. (a) 9CoNi-A at 1000 °C/500 h; (b) 9CoNi-B at 1000 °C/500 h; (c) 9CoNi-C at 950 °C/600 h; (d) 9CoNi-C at 950 °C/600 h.

2.2.2. Oxidation and Mechanical Properties

**Figure 4** shows the oxidation and mechanical properties of the predicted novenary alloys. The oxidation weight gain shown in Figure 4(a) indicates that all four novenary alloys have better oxidation resistance than the Cr-free γ′-strengthened Co-based superalloys with a fewer components after 1000 °C/100 h. The weight gain of the four novenary alloys decreases in the order of 9CoNi-C>9CoNi-A>9CoNi-D≈9CoNi-B. The oxidation resistance of alloys 9CoNi-B and 9CoNi-D is close to that of typical Ni-based superalloys CMSX-4 and CMSX-6. The oxidation behavior strongly depends on the interaction of Al and Cr, which has been studied and shown in our previous works.[19][56] The Vickers hardness of the four novenary alloys at room temperature increases in the order of 9CoNi-A<9CoNi-B<9CoNi-C<9CoNi-D, as shown in Figure 4(b). Interestingly, the

This article is protected by copyright. All rights reserved

Accepted Article

15272648, 2023, 0, Downloaded from https://onlinelibrary.wiley.com. By MPI 337 Iron Research - on 02. Februar 2023. Re-use and distribution is strictly not permitted, except for Open Access articles

variation of Vickers hardness seems to not be closely related to the $A_{\gamma'}$. For example, although the alloy 9CoNi-A has the highest $A_{\gamma'}$ among the four novenary alloys, its Vickers hardness is lower than the other three alloys. In contrast, for the industrial gas turbine alloys 9CoNi-C and 9CoNi-D, the variation of Vickers hardness is positively correlated with the $A_{\gamma'}$. This will be further discussed in the following sections.

Figure 4(c) shows 0.2% flow stress curves as a function of temperature for single crystal alloys 9CoNi-A and 9CoNi-D, together with other single crystal CoNi-based alloys with fewer components (≤6),[53][60] and Co-Al-W-based alloy.[40] In the whole temperature range, the flow stresses of alloy 9CoNi-D are higher than that of 9CoNi-A. Alloy 9CoNi-A presents an anomalous yield behavior and has a higher or comparable yield strength at 800 °C compared to the CoNi- and Co-Al-W-based alloys with high W content (≥4 at. %). Above 800 °C, its flow stress decreases rapidly as it does for other CoNi- and Co-Al-W-based alloys. In contrast, with the increase of temperature, the flow stresses of alloy 9CoNi-D decrease without the anomalous yield behavior. Even so, the alloy 9CoNi-D shows higher flow stresses at temperatures below 800°C than other reported CoNi- or Co-Al-W-based alloys.

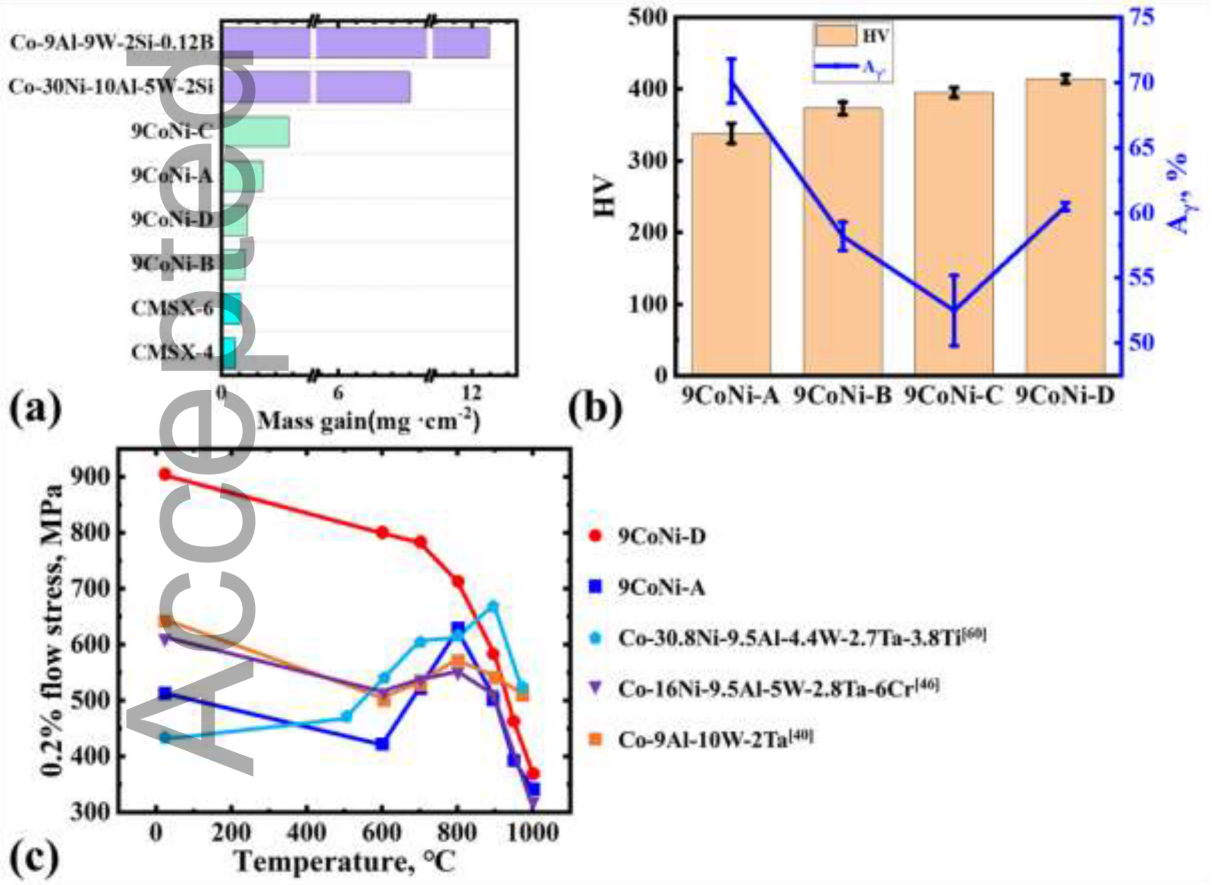


**Figure 4.** The oxidation and mechanical properties of four novenary alloys. (a) Comparison of oxidation weight gains between γ′-strengthened Co-based and Ni-based superalloys after 1000 °C/100 h; (b) Vickers hardness and the corresponding $A_{\gamma'}$; (c) 0.2% flow stress curves as a

This article is protected by copyright. All rights reserved

15272648, 2023, 0, Downloaded from https://onlinelibrary.wiley.com. By MPI 337 Iron Research - on 02. Februar 2023. Re-use and distribution is strictly not permitted, except for Open Access articles

Accepted Article

function of temperature for single crystal alloys 9CoNi-A and 9CoNi-D, together with other single crystal CoNi-based alloys with lower components (≤6),[53][60] and Co-Al-W-based alloy[40].

### 2.3. Comparison between Machine-Learning and CALPHAD

The synergetic effects of multiple elements have always been one of the key issues for the design of superalloys. The rapid and accurate establishment of a quantitative relationship between multiple elements and microstructure will greatly accelerate the development of new alloys. Therefore, many researches have been done to build thermodynamic and kinetic databases of γ′-strengthened Co-based superalloys.[61][62] Moreover, some CoNi-based superalloys with good microstructural stability and mechanical properties have been developed through the CALPHAD.[11][13] Even so, due to the complexity of the synergetic effects of multiple elements, the existing CALPHAD cannot effectively predict all the microstructural properties, especially for the (γ+γ′)/(γ+γ′+TCP) phase boundaries in multicomponent alloys.[26] Compared with the CALPHAD, multicomponent diffusion-multiples can quickly obtain experimental data for the composition and corresponding microstructure. This brings an advantage in determining the phase boundaries of an alloy system.[26][34] The machine-learning method can establish the digital or functional relationship among multiple elements, microstructures and properties. However, its extrapolation is limited due to the lack of an understandable physical metallurgy principle. In addition, high-quality data is required during the model training process to ensure the accuracy of predictions. Therefore, combined with the large high-quality experimental database provided by the multicomponent diffusion-multiple, it is expected to significantly improve the accuracy of machine-learning predictions.

**Figure 5** shows the pseudo ternary isothermal section of alloy Co-Al-W-20Ni-1Ta-4Ti (at. %) calculated by phase diagram at 1000 °C and a comparison between the experimental data from the diffusion-multiples and the predicted data by the machine-learning model. The CALPHAD result shows that four phase regions, including γ, γ+γ′, γ+γ′+β and γ+β, exist in the composition range of 7%≤ Al ≤ 15%, 0%≤ W ≤ 8% (at. %). The γ/γ+γ′ phase boundary is similar between the experimental data and CALPHAD. However, there exists an apparent deviation (~2at. %) for the γ+γ′/γ+γ′+β boundary, as shown in Figure 5(a). In contrast, the machine-learning prediction results (Figure 5(b)) show a better fitness with the actual experimental results (Figure 5(a)) than the CALPHAD. Thus, it can be summarized that the machine-learning model based on the experimental data is more accurate than CALPHAD in predicting the phase constituent, especially when the phase boundary is contained. Besides the prediction of phase constituent, taking advantage of experimental data, the machine-learning model also has higher accuracy than CALPHAD when predicting the $T_{\gamma'}$ and $A_{\gamma'}$ in the database (not shown in this study).

This article is protected by copyright. All rights reserved

Accepted Article

15272648, 2023, 0, Downloaded from https://onlinelibrary.wiley.com. By MPI 337 Iron Research - on 02. Februar 2023. Re-use and distribution is strictly not permitted, except for Open Access articles

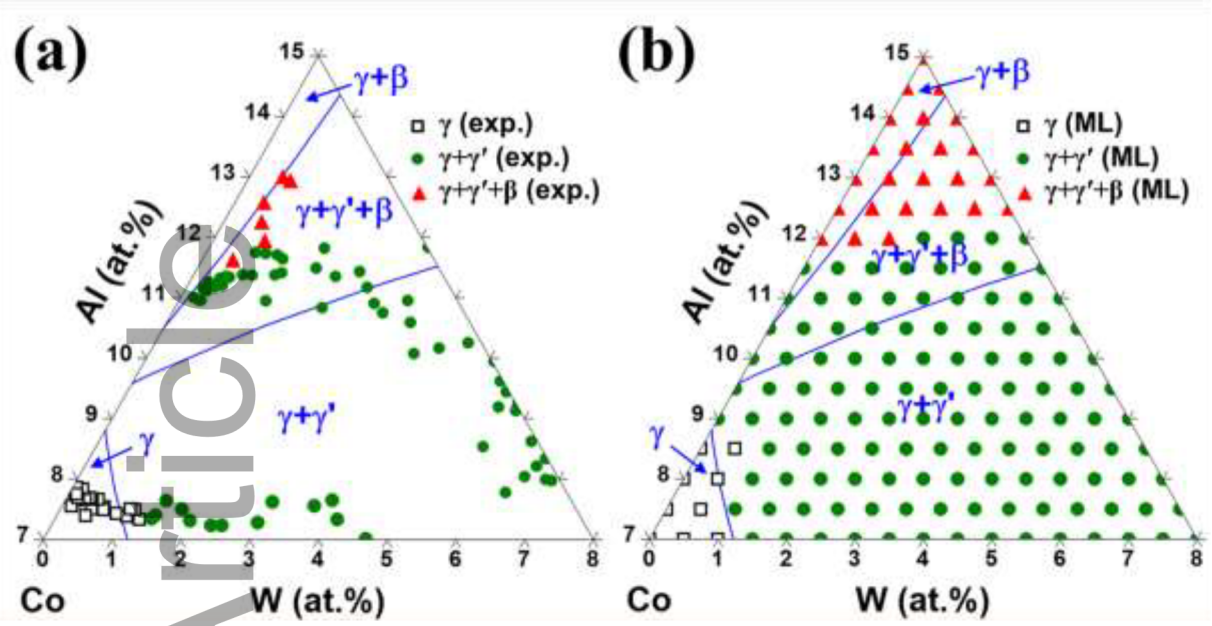


**Figure 5.** The pseudo ternary isothermal section of alloy Co-Al-W-20Ni-1Ta-4Ti (at. %) calculated by phase diagram at 1000 °C and a comparison between (a) the experimental data from the diffusion-multiples and (b) the predicted data by the machine-learning model.

Despite high-accuracy databases, the limited extrapolation out of the database has always been a critical issue for machine-learning models. To solve this problem, additional key experimental tests are generally performed and fed into the database, then the machine-learning models are re-trained.[11][27][29] A similar process will be repeated until an acceptable predicted result is obtained. For example, the range of A element in a database of the machine-learning models is 0~10 at. %. It is difficult to ensure good accuracy for predicting the alloys with a content of 10~20 at. %A unless the supplement of extra experimental data, like alloys with ≥20 at. %A, into the previous database. Meanwhile, to avoid overfitting, some experimental data of alloys with 10~20 at. %A is also required.

### 2.4. "Cross-Component" Prediction from Low to High-Component γ′-Strengthened Co-Based Superalloys

Based on the aforementioned principles, the alloys in the database and predictions of the machine-learning models typically contain the same number of components. Thus, it seems impossible to make a "cross-component" prediction, in which the high-component alloys are predicted based on data from the low-component alloys in the database. However, the volume of extra experiments may be unacceptable because of the complexity of the synergetic effects of multiple elements, especially for the prediction of high-component (>7) alloys. Moreover, it is difficult for researchers to handle the

This article is protected by copyright. All rights reserved

Accepted Article

15272648, 2023, 0, Downloaded from https://onlinelibrary.wiley.com. By MPI 337 Iron Research - on 02. Februar 2023. Re-use and distribution is strictly not permitted, except for Open Access articles

data about simultaneous variations of complex elements. On the other hand, the prediction results of CALPHAD or "CALPHAD + machine-learning" strongly depend on the accuracy of built-in thermodynamic databases, which are uncertain or unavailable for γ′-strengthened Co-based superalloys with high components (>7) for now[11].

2.4.1. Feasibility of "diffusion-multiple + machine-learning" method to Make "Cross-Component" Prediction

The diffusion-multiple has a unique advantage in establishing the experimental database. Theoretically, any synergetic effects of multiple elements can be easily obtained by designing the corresponding diffusion couples. Thus, it is ideal for the combination of diffusion-multiple and machine-learning models to improve the reliability of prediction for the high-component γ′-strengthened Co-based superalloys. In addition, to make full use of the advantage of machine learning in processing multi-dimensional data and reduce the costs of experiments, in the current research, the high-precision experimental data provided by the diffusion-multiple mainly came from alloys with 6~7 components. All the elements of the novenary alloys shown in Table 2 are contained by overlapping two or more diffusion couples, thus realizing a "pseudo coverage" to meet the principle of machine-learning prediction. Therefore, novenary alloys can be predicated by simulating or fitting the synergetic effects of multiple elements using machine-learning models.

In this study, the four novenary alloys shown in Table 2 have a γ+γ′ configuration at 950~1000 °C and good oxidation resistance at 1000 °C. These mean a good accuracy in the phase constituent prediction and validity of the criterion set for the oxidation property (Table 1). **Figure 6** shows the comparisons of $T_{\gamma'}$ and $A_{\gamma'}$ values among the CALPHAD, machine-learning (MC) and experimental (TEST) results of four novenary superalloys. In terms of the $T_{\gamma'}$, the machine-learning results show comparable or slightly higher accuracy than CALPHAD, as shown in Figure 6(a). The absolute deviations of $T_{\gamma'}$ between the machine-learning and experimental results are lower than 20 °C, while the minimum deviation of CALPHAD results is 24 °C for alloys 9CoNi-A, 9CoNi-B, and 9CoNi-C. For the $T_{\gamma'}$ of alloy 9CoNi-D, both methods show a lower accuracy, a deviation larger than 30 °C compared to the experimental value.

The $A_{\gamma'}$ results of the four novenary alloys shown in Figure 6(b) indicate that the trends predicted by the two methods are similar to the variation of experimental values. At the same time, their prediction accuracy is different. The machine-learning result of alloy 9CoNi-A is comparable or slightly closer to the experimental value than the CALPHAD. On the contrary, CALPHAD tends to be favorable for the other three novenary alloys. However, all the experimental $A_{\gamma'}$ values of alloys 9CoNi-B, 9CoNi-C and 9CoNi-D are lower than the design criteria shown in Table 1. This is closely

This article is protected by copyright. All rights reserved

Accepted Article

15272648, 2023, 0, Downloaded from https://onlinelibrary.wiley.com. By MPI 337 Iron Research - on 02. Februar 2023. Re-use and distribution is strictly not permitted, except for Open Access articles

related to the database used for the $A_{\gamma'}$ prediction. The diffusion couples shown in Figures 2(a) and (b) mainly (>80%) have a lower Cr content (≤6 at. %). As such, the database for the machine-learning model is sufficient to make a good "cross-component" prediction on the $A_{\gamma'}$ of alloy 9CoNi-A with 4 at. %Cr. In contrast, the machine-learning predicts the $A_{\gamma'}$ of alloys 9CoNi-B~D (7~14 at. %Cr) with a large deviation due to the lack of $A_{\gamma'}$ data with high Cr content. In contrast, the thermodynamic database-dependent CALPHAD is equipped with simulation data from high to low Cr contents. Although it is not enough to give a high-precise prediction, the trend is still meaningful for the design of novel alloys, especially when no experimental data is available.

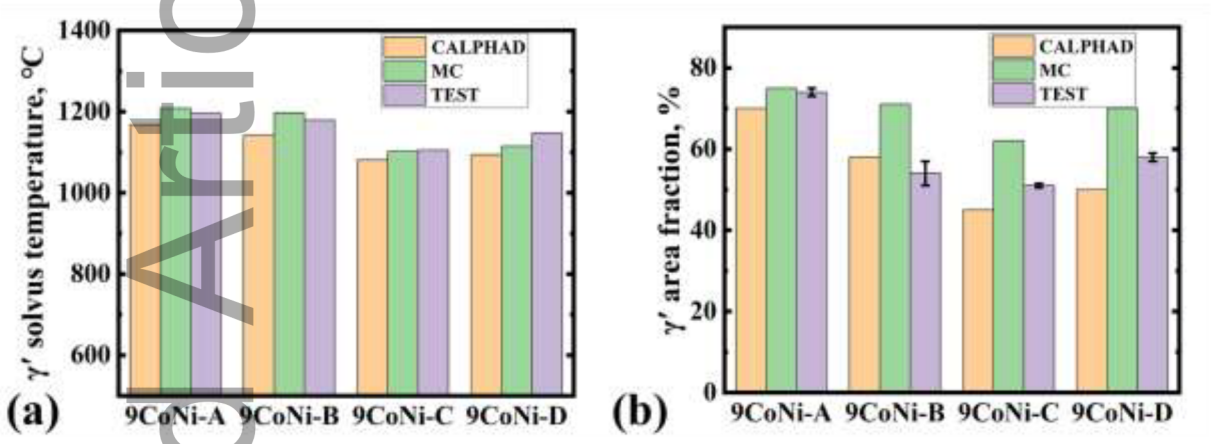


**Figure 6.** Comparison of (a) $T_{\gamma'}$ and (b) $A_{\gamma'}$ values among the CALPHAD, machine-learning and experimental results of four novenary γ′-strengthened Co-based superalloys.

2.4.2. Features of "diffusion-multiple + machine-learning" Method

Based on the above comparison, it can be summarized that the accuracy of the "diffusion-multiple + machine-learning" method strongly depends on the experimental data. Although all the individual diffusion couples have been combined to improve the "cross-component" predictable capability, a compositional boundary still exists. The prediction accuracy near or outside the boundary decreases rapidly, such as alloys 9CoNi-B~D. Even so, it should be noted that the aforementioned composition range is in the alloys with fewer components (6~7), not the novenary alloys. The prediction results of alloy 9CoNi-A have proved the feasibility for the "cross-component" prediction by the "diffusion-multiple + machine-learning" method based on a large number of high-quality experimental data and searching for the candidates that match the designing criteria. Additionally, as discussed in Figure 5, the diffusion couple has the advantage of determining the (γ+γ′)/(γ+γ′+detrimental phase) boundary more accurately than the CALPHAD method, which is highly important for the design of high-component alloys. This has been further evidenced by a design process based on the "CALPHAD + machine-learning" method in our previous work, where most predicted 7-component alloys precipitated the detrimental phases due to the low accuracy of the phase

This article is protected by copyright. All rights reserved

Accepted Article

15272648, 2023, 0, Downloaded from https://onlinelibrary.wiley.com. By MPI 337 Iron Research - on 02. Februar 2023. Re-use and distribution is strictly not permitted, except for Open Access articles

boundaries only using thermodynamic calculation data.[11] For the prediction of $A_{\gamma'}$ shown in Figure 6(b), the "diffusion-multiple + machine-learning" method shows a lower accuracy than the CALPHAD and only maintains a trend prediction. However, it should be noted that building the thermodynamic database is a giant project, especially for the high-component alloy with refractory elements. Many thermodynamic parameters, such as Gibbs free energy, Entropy and Enthalpy, are required to obtain a reasonable accuracy. Moreover, for different thermodynamic databases and objective alloy systems, the deviation between the experimental and prediction results may be unacceptable. In this study, besides the advantage in determining phase boundaries, the "diffusion-multiple + machine-learning" method is mainly constructed from multiple algorithms, which can rapidly build the mapping relation between multiple elements and thermodynamic properties based on the sufficient experimental dataset instead of the sluggish calculation for the fundamental thermodynamic parameters from numerous low-component alloys. Complex synergetic effects of multiple elements can be predicted by machine-learning algorithms, and optimal selections can be screened based on the existing experimental results. This has been verified to be feasible for designing novel alloy systems[27][29][30] or widely reported Ni-based superalloys.[28]

Even so, some critical issues still need to be pointed out for the "cross-component" prediction method in this study. (1) Similar to the other machine-learning method, the quality and quantity of data are the most critical factors for prediction accuracy. (2) The composition of predicted alloys should be included within the composition range of the database as far as possible, especially for the elements having a significant impact on the microstructure and properties, such as Cr. (3) Compared with CALPHAD, the predictions beyond the scope of the database, and the interaction between multiple elements are the key problems for the machine-learning method. Making full use of the advantage of diffusion-multiples and supplementing the critical experimental data of the low-component alloys should be a solution to improve the accuracy and capability of "cross-component" prediction. For example, only four novenary alloys are verified in this study, and the content of Mo and Nb may be too low to affect the phase constituent of the novenary alloy. Therefore, the supplementary data containing both Mo and Nb elements will be helpful to improve the validity of machine-learning models for predicting the existing four novenary alloys and the high-component alloys with higher Mo and Nb contents in the future. Moreover, the advantage of the diffusion-couple in predicting the detrimental phase boundaries will be more critical when more or higher content of refractory elements are considered in the design criteria. A large number of alloys with lower Cr contents in the diffusion-multiple contribute to the high prediction accuracy for the alloy 9CoNi-A. For the other three alloys, it is expected to be able to improve the performance of the machine-learning model for the $A_{\gamma'}$ by supplementing the database with more data of high Cr alloys.

This article is protected by copyright. All rights reserved

Accepted Article

15272648, 2023, 0, Downloaded from https://onlinelibrary.wiley.com. By MPI 337 Iron Research - on 02. Februar 2023. Re-use and distribution is strictly not permitted, except for Open Access articles

15272648, 2023, 0, Downloaded from https://onlinelibrary.wiley.com. By MPI 337 Iron Research - on 02. Februar 2023. Re-use and distribution is strictly not permitted, except for Open Access articles

Accepted Article

### 2.5. Relationship between the Composition and Mechanical Properties

Vickers hardness and compressive strength are two important and widely studied mechanical properties, which can be easily obtained and reflect other mechanical performances of superalloys to a certain extent. They represent a comprehensive effect of various strengthening mechanisms in the alloy, such as solution and precipitation.[28] Thus, it can sometimes be used as one of the criteria for evaluating superalloys. The strengthening of γ′ precipitation is one of the most important strengthening mechanisms in superalloys. To improve its stability, the question of how to expand the γ+γ′ phase region and improve the $T_{\gamma'}$ has always been a key issue for the development of γ′-strengthened Co-based superalloys. Combined with the results in this study, during the design process of alloys 9CoNi-A and 9CoNi-B, higher $T_{\gamma'}$ is demanded to obtain a higher $A_{\gamma'}$ at high temperatures. In contrast, for alloys 9CoNi-C and 9CoNi-D, the corrosion resistance seems to be more important than the $T_{\gamma'}$ due to the severe corrosion environment and lower service temperature than the aero-engines. Thus, a high Cr content (>12 at. %) is set as the design criteria of industrial gas turbine alloys (Table 1). In addition, the effect of solution strengthening is also a critical factor that cannot be neglected. As shown in Figure 4(b), although the $A_{\gamma'}$ of alloy 9CoNi-A (~70%) is obviously higher than that of 9CoNi-B (~58%), the variation of Vickers hardness shows the opposite trend. This can be ascribed to the comprehensive effect between the solution and precipitation strengthening. In terms of composition, the alloy 9CoNi-B is different from alloy 9CoNi-A by the lower Al+Ti and higher Cr contents. The former contributes to the precipitation strengthening effect as γ′-forming elements, while the latter enhances the solution strengthening of the matrix, due to the larger atomic radius compared to Co, and decreases the $A_{\gamma'}$. Therefore, the effect of solution strengthening is more dominant on the Vickers hardness than the γ′ precipitation for alloys 9CoNi-A and 9CoNi-B. In contrast, the precipitation strengthening seems to be dominant for the Vickers hardness of alloys 9CoNi-C and 9CoNi-D. Although the solution strengthening elements in alloy 9CoNi-C (W+Mo+Cr=17.5 at. %) is higher than that in alloy 9CoNi-D (14.5 at. %), the Vickers hardness of alloy 9CoNi-D (HV=~414) with a higher $A_{\gamma'}$ (~62%) was slightly higher than that of alloy 9CoNi-C ($A_{\gamma'}$=~52%, HV=~395). Indeed, for the four novenary alloys, the variation of Vickers hardness is more related to the sum of solution strengthening elements in order of 9CoNi-$A_{W+Mo+Cr=6.5\ at.\ \%}$<9CoNi-$B_{W+Mo+Cr=9.5\ at.\ \%}$<9CoNi-$C_{W+Mo+Cr=14.5\ at.\ \%}$<9CoNi-$D_{W+Mo+Cr=17.5\ at.\ \%}$. A similar trend was also observed when comparing the compressive flow stress of alloys 9CoNi-A and 9CoNi-D (Figure 4(c)). Especially, the solution strengthening effect plays a more critical role than the $A_{\gamma'}$ at the temperatures below 800 °C. While at higher temperatures (>800 °C), the influence of precipitation

This article is protected by copyright. All rights reserved

strengthening on the mechanical property increases and the deviation of flow stress between the alloys 9CoNi-A and 9CoNi-D decreases.

Based on the relationship between the content of solution strengthening elements, $A_{\gamma'}$, Vickers hardness and compressive property, to obtain good mechanical properties, the solution strengthening effect should also be contained in the design criteria besides the $A_{\gamma'}$. For example, the impact of solution strengthening in alloy 9CoNi-A needs to be enhanced when higher values of Vickers hardness and flow stress are expected. In addition, the misfit between γ and γ′ phases is not considered in this study, which has a significant influence on the coarsening of γ′ precipitates and creep resistance at high temperatures. For example, alloy 9CoNi-B may have a higher misfit value compared to the alloy 9CoNi-A as estimated by the coarsening of γ′ precipitates at 1000 °C/500 h (Figures 3(a) and (b)). Therefore, this is another factor that needs to be considered for optimizing the design criteria in the future. Accordingly, the corresponding machine-learning models should also be developed and applied.

## 3. Conclusions

We propose a "cross-component" prediction method for the high-component (>7) γ′-strengthened Co-based superalloys by integrating the experimental data from diffusion-multiples assembled by a series of diffusion couples with low number of components and machine-learning models. Four novenary alloys were screened out according to the different design criteria for the aero-engine and industrial gas turbine blades. These alloys show good microstructural stability at 950~1000 °C and oxidation resistance at 1000 °C. Compared with a CALPHAD approach, the "diffusion-multiple + machine-learning" method has been verified to reach a comparable or slightly higher accuracy for the $T_{\gamma'}$ of high-component alloys, such as alloy 9CoNi-A, when enough related data from low-component diffusion couples is provided. In contrast, the trend prediction by the CALPHAD is still meaningful, especially when the related experimental data is deficient. Expanding the compositional range in the database and supplementing the critical interaction data of multiple elements are beneficial for improving the prediction accuracy of the "cross-component" machine-learning models. As indicated by the microstructural stability, compression test, and Vickers hardness results, the influence of solution strengthening and γ/γ′ misfit should also be considered for the establishment of machine-learning model and design criteria to further improve mechanical properties in the future.

## 4. Experimental Section

This article is protected by copyright. All rights reserved

Accepted Article

15272648, 2023, 0, Downloaded from https://onlinelibrary.wiley.com. By MPI 337 Iron Research - on 02. Februar 2023. Re-use and distribution is strictly not permitted, except for Open Access articles

*Thermodynamic analysis:* All the thermodynamic calculations of phase constituent, $T_{\gamma'}$ and $A_{\gamma'}=(V_{\gamma'})^{2/3}$[37][63] in this study were performed using the PANDAT software with the commercial Co-based thermodynamic database PanCo2018.

*Machine-learning model fitting:* Widely used 10-fold cross validation[64] was used to avoid overfitting of the selected models. First, the whole dataset was scrambled and divided randomly into 10 subsets. Then, one subset would be used as the testing set, while the other nine subsets would be used as the training set. Finally, the training set was fed into different algorithms to build machine-learning models. This process would cycle 10 times, where each subset would be used as testing set exactly once. The brute-force grid search algorithm was employed to optimize and tune parameters for machine-learning models.

*Diffusion-multiple preparations*: All the individual experimental alloys in the diffusion-multiple were prepared by arc-melting high-purity (>99.9 wt. %) elements in an argon atmosphere and sectioned into blocks to assemble a collection of diffusion couples. Then, the diffusion-multiple was treated by hot isostatic pressing (HIP) at 1200 °C/160 MPa for 5 h to achieve good interfacial contact among the alloy pieces. After that, the diffusion-multiple was heat treated in the following process: 1250 °C/24 h + 1000 °C/1000 h. More details can be referred to the literature.[21][26][34]

*Single crystal superalloys preparations*: All the single crystal alloys were melted in a vacuum induction furnace, and subsequently directionally solidified into [001]-oriented single crystal rods with a diameter of 15 mm and a length of ~170 mm, using the conventional Bridgman method. Then the heat-treatment process of single crystal rods was set as 1230 ℃/12 h +1000 ℃/24 h+800 ℃/16 h for the alloy 9CoNi-A, and 1250 ℃/12 h +1000 ℃/4 h+800 ℃/16 h for the alloy 9CoNi-D.

*Compositional measurements*: Composition profiles across the diffusion couple were obtained using quantitative electron probe microanalysis (EPMA) on a JEOL JXA8230 microprobe at an accelerating voltage of 20 kV with a probe current of 10 nA. The beam spot diameter and the step size of each EPMA spot were both set as 5 μm.

*Physical, Oxidation and Mechanical properties*: Cylindrical samples of 3 mm diameter and 1.5 mm thickness were cut for differential scanning calorimetry (DSC) experiments. Then, the $T_{\gamma'}$ was determined by the NETZSCH STA 449C thermal analyzer under high purity Ar flow with a heating rate of 10 °C $min^{-1}$. The hardness was measured using an HXD-1000TM Vickers hardness testing system with a load of 200 g and a dwell time of 10 s. The final value of Vickers hardness (HV) was obtained by averaging the results from five cycles. The density was measured using a water displacement approach based on the Archimedes principle. Isothermal oxidation tests were carried out at 1000 ℃/100 h in air. Mass gains were measured by analytical balance with an accuracy of $10^{-4}$ g. Compressive specimens with [001] orientation (<10° deviation) were machined from heat-treated

This article is protected by copyright. All rights reserved

Accepted Article

15272648, 2023, 0, Downloaded from https://onlinelibrary.wiley.com. By MPI 337 Iron Research - on 02. Februar 2023. Re-use and distribution is strictly not permitted, except for Open Access articles

samples with a gauge length of 7.5 mm and a diameter of 5 mm. Compressive tests were conducted at room temperature, 600 °C, 700 °C, 800 °C, 900 °C, 950 °C and 1000 °C with a strain rate of $10^{-4}$ $s^{-1}$.

*Microstructural characterizations*: The metallographic specimens of diffusion couples and ingots were prepared using standard metallographic sample preparation techniques and etched in a solution of 1% HF + 33% $HNO_3$ + 33% $CH_3COOH$ + 33% $H_2O$ (by volume). The microstructure was characterized by the ZEISS SUPRA 55 field-emission scanning electron microscope. The γ′ area fraction ($A_{\gamma'}$) corresponding to each composition spot was measured within a rectangle having a size of 5 μm × 400 μm (the length is parallel to the interface of the diffusion couple) by the standard point count method.

## Supporting Information

Supporting Information is available from the Wiley Online Library or the author.

## Conflict of Interest

The authors declare no conflict of interest.

## Acknowledgments

The authors would like to thank Ji-Cheng Zhao for the assistance in the design of diffusion-multiples. This research was supported by the National Natural Science Foundation of China (Grant No.: 52171095, 52201100, 52201024 and 92060113), China Postdoctoral Science Foundation (Grant No.: 2022M710346), Science and Technology on Advanced High Temperature Structural Materials Laboratory (Grant No.: 6142903210207), Natural Science Foundation of Hunan Province (Grant No.: 2022JJ40441), National Key Research and Development Program of China (Grant No.: 2017YFB0702902) and Key-Area Research and Development Program of Guangdong Province (Grant No.: 2019B010943001).

## References

[1] J. Sato, T. Omori, K. Oikawa, I. Ohnuma, R. Kainuma, K. Ishida, *Science*. **2006**, *312*, 90.

[2] C.S. Lee, *Precipitation-Hardening Characteristics of Ternary Cobalt-Aluminum-X Alloys*, The University of Arizona, **1971**.

Accepted Article

15272648, 2023, 0, Downloaded from https://onlinelibrary.wiley.com. By MPI 337 Iron Research - on 02. Februar 2023. Re-use and distribution is strictly not permitted, except for Open Access articles

This article is protected by copyright. All rights reserved

[3] T.M. Pollock, J. Dibbern, M. Tsunekane, J. Zhu, A. Suzuki, *J. Miner. Met. Mater. Soc.* **2010**, *62*, 58.

[4] A. Suzuki, H. Inui, T.M. Pollock, *Annu. Rev. Mater. Res.* **2015**, *45*, 345.

[5] R.C. Reed, *The Superalloys Fundamentals and Applications*, Cambridge University Press, Cambridge **2006**.

[6] M.S. Titus, Y.M. Eggeler, A. Suzuki, T.M. Pollock, *Acta Mater.* **2015**, *82*, 530.

[7] A. Bauer, S. Neumeier, F. Pyczak, M. Göken, *Adv. Eng. Mater.* **2014**, *17*, 748.

[8] F. Xue, H.J. Zhou, X.F. Ding, M.L. Wang, Q. Feng, *Mater. Lett.* **2013**, *112*, 215.

[9] S. Neumeier, L.P. Freund, M. Göken, *Scr. Mater.* **2015**, *109*, 104.

[10] E.A. Lass, D.J. Sauza, D.C. Dunand, D.N. Seidman, *Acta Mater.* **2018**, *147*, 284.

[11] P. Liu, H. Huang, S. Antonov, C. Wen, D. Xue, H. Chen, L. Li, Q. Feng, T. Omori, Y. Su, *Npj Comput. Mater.* **2020**, *6*, 1.

[12] K. Shinagawa, T. Omori, J. Sato, K. Oikawa, I. Ohnuma, R. Kainuma, K. Ishida, *Mater. Trans.* **2008**, *49*, 1474.

[13] W. Li, L. Li, S. Antonov, Q. Feng, *Mater. Des.* **2019**, *180*, 107912.

[14] L. Shi, J.J. Yu, C.Y. Cui, X.F. Sun, *Mater. Sci. Eng. A.* **2015**, *635*, 50.

[15] A. Bauer, S. Neumeier, F. Pyczak, M. Göken, *Scr. Mater.* **2010**, *63*, 1197.

[16] M. Ooshima, K. Tanaka, N.L. Okamoto, K. Kishida, H. Inui, *J. Alloys Compd.* **2010**, *508*, 71.

[17] L. Lilensten, P. Kürnsteiner, J.R. Mianroodi, A. Cervellon, J. Moverare, M. Segersäll, S. Antonov, P. Kontis, in *Superalloys 2020* (Eds: S. Tin, M. Hardy, J. Clews, J. Cormier, Q. Feng, J. Marcin, C. O'Brien, A. Suzuki), John Wiley & Sons, Inc. **2020**, 41.

[18] S. Antonov, W. Chen, S. Lu, D. Isheim, D.N. Seidman, Q. Feng, E. Sun, S. Tin, *Scr. Mater.* **2019**, *161*, 44.

[19] W. Li, L. Li, S. Antonov, F. Lu, Q. Feng, *J. Alloys Compd.* **2020**, *826*, 154182.

[20] L. Klein, Y. Shen, M.S. Killian, S. Virtanen, *Corros. Sci.* **2011**, *53*, 2713.

[21] M. Zou, W. Li, L. Li, J.-C. Zhao, Q. Feng, in *Superalloys 2020* (Eds: S. Tin, M. Hardy, J. Clews, J. Cormier, Q. Feng, J. Marcin, C. O'Brien, A. Suzuki), John Wiley & Sons, Inc. **2020**, 937.

[22] S. Lu, S. Antonov, L.F. Li, C.P. Liu, X.N. Zhang, Y.F. Zheng, H.L. Fraser, Q. Feng, *Acta Mater.* **2020**, *190*, 16.

[23] P. Pandey, A.K. Sawant, B. Nithin, Z. Peng, S.K. Makineni, B. Gault, K. Chattopadhyay, *Acta Mater.* **2019**, *168*, 37.

[24] N. Volz, C.H. Zenk, R. Cherukuri, T. Kalfhaus, M. Weiser, S.K. Makineni, C. Betzing, M. Lenz, B. Gault, S.G. Fries, J. Schreuer, R. Vaßen, S. Virtanen, D. Raabe, E. Spiecker, S. Neumeier, M. Göken, *Metall. Mater. Trans. A.* **2018**, *49*, 4099.

This article is protected by copyright. All rights reserved

Accepted Article

15272648, 2023, 0, Downloaded from https://onlinelibrary.wiley.com. By MPI 337 Iron Research - on 02. Februar 2023. Re-use and distribution is strictly not permitted, except for Open Access articles

[25] E.A. Lass, Metall. *Mater. Trans. A.* **2017**, *48*, 2443.

[26] W. Li, L. Li, C. Wei, J.-C. Zhao, Q. Feng, *J. Mater. Sci. Technol.* **2021**, *80*, 139.

[27] J. Yu, C. Wang, Y. Chen, C. Wang, X. Liu, *Mater. Des.* **2020**, *195*, 108996.

[28] N. Khatavkar, S. Swetlana, A.K. Singh, *Acta Mater.* **2020**, *196*, 295.

[29] J. Yu, S. Guo, Y. Chen, J. Han, Y. Lu, Q. Jiang, C. Wang, X. Liu, *Intermetallics.* **2019**, *110*, 106466.

[30] J. Ruan, W. Xu, T. Yang, J. Yu, S. Yang, J. Luan, T. Omori, C. Wang, R. Kainuma, K. Ishida, C.T. Liu, X. Liu, *Acta Mater.* **2020**, *186*, 425.

[31] Y. Mishin, *Acta Mater.* **2021**, *214*, 116980.

[32] J.C. Zhao, Z. Xuan, D.G. Cahill, *Mater. Today*, **2005**, *8*, 28.

[33] L. Zhu, C. Wei, H. Qi, L. Jiang, Z. Jin, J.-C. Zhao, *J. Alloys Compd.* **2016**, *691*, 110.

[34] W. Li, L. Li, S. Antonov, C. Wei, J.-C. Zhao, Q. Feng, *J. Alloys Compd.* **2021**, *881*, 160618.

[35] J. Opitz, S. Burst, *ArXiv Prepr. ArXiv191103347*. **2019**.

[36] F. Xue, H.J. Zhou, Q.Y. Shi, X.H. Chen, H. Chang, M.L. Wang, Q. Feng, *Scr. Mater.* **2015**, *97*, 37.

[37] S. Lu, S. Antonov, L.F. Li, Q. Feng, *Metall. Mater. Trans. A.* **2018**, *49*, 4079.

[38] J. He, M. Zou, L. Li, X. Wang, Q. Feng, *Mater. Lett.* **2020**, *262*, 127042.

[39] F. Xue, M.L. Wang, Q. Feng, in *Superalloys 2012* (Eds: Eric S. Huron, Roger C. Reed, Mark C. Hardy, Michael J. Mills, Rick E. Montero, Pedro D. Portella, Jack Telesman), TMS, **2012**, 813.

[40] A. Suzuki, T.M. Pollock, *Acta Mater.* **2008**, *56*, 1288.

[41] M.S. Titus, *High Temperature Deformation Mechanisms of $L1_2$-Containing Co-Based Superalloys*, University of California Santa Barbara, **2015**.

[42] A. Bauer, S. Neumeier, F. Pyczak, M. Göken, in *Superalloys 2012* (Eds: Eric S. Huron, Roger C. Reed, Mark C. Hardy, Michael J. Mills, Rick E. Montero, Pedro D. Portella, Jack Telesman), TMS, **2012**, 695.

[43] C.H. Zenk, A. Bauer, P. Goik, S. Neumeier, H.J. Stone, M. Göken, *Metall. Mater. Trans. A.* **2016**, *47*, 2141.

[44] M. Weiser, M.C. Galetz, H.-E. Zschau, C.H. Zenk, S. Neumeier, M. Göken, S. Virtanen, *Corros. Sci.* **2019**, *156*, 84.

[45] N. Volz, F. Xue, A. Bezold, C.H. Zenk, S.G. Fries, J. Schreuer, S. Neumeier, M. Göken, Metall. *Mater. Trans. A.* **2021**, *52*, 3931.

[46] L. Shi, J.J. Yu, C.Y. Cui, X.F. Sun, *Mater. Lett.* **2015**, *149*, 58.

[47] M. Knop, P. Mulvey, F. Ismail, A. Radecka, K.M. Rahman, T.C. Lindley, B.A. Shollock, M.C. Hardy, M.P. Moody, T.L. Martin, P.A.J. Bagot, D. Dye, *JOM.* **2014**, *66*, 2495.

This article is protected by copyright. All rights reserved

Accepted Article

15272648, 2023, 0, Downloaded from https://onlinelibrary.wiley.com. By MPI 337 Iron Research - on 02. Februar 2023. Re-use and distribution is strictly not permitted, except for Open Access articles

[48] T. Omori, K. Oikawa, J. Sato, I. Ohnuma, U.R. Kattner, R. Kainuma, K. Ishida, *Intermetallics.* **2013**, *32*, 274.

[49] S. Kobayashi, Y. Tsukamoto, T. Takasugi, *Intermetallics.* **2011**, *19*, 1908.

[50] S. Meher, H.Y. Yan, S. Nag, D. Dye, R. Banerjee, *Scr. Mater.* **2012**, *67*, 850.

[51] H.-Y. Yan, J. Coakley, V.A. Vorontsov, N.G. Jones, H.J. Stone, D. Dye, *Mater. Sci. Eng. A.* **2014**, *613*, 201.

[52] F. Pyczak, A. Bauer, M. Göken, U. Lorenz, S. Neumeier, M. Oehring, J. Paul, N. Schell, A. Schreyer, A. Stark, F. Symanzik, *J. Alloys Compd.* **2015**, *632*, 110.

[53] H.Y. Yan, V.A. Vorontsov, J. Coakley, N.G. Jones, H.J. Stone, D. Dye, in *Superalloys 2012* (Eds: Eric S. Huron, Roger C. Reed, Mark C. Hardy, Michael J. Mills, Rick E. Montero, Pedro D. Portella, Jack Telesman), TMS, **2012**, 705.

[54] T.M. Pollock, S. Tin, *J. Propuls. Power.* **2006**, *22*, 361.

[55] T. Murakumo, T. Kobayashi, Y. Koizumi, H. Harada, *Acta Mater.* **2004**, *52*, 3737.

[56] X. Zhuang, L. Li, Q. Feng, in *Superalloys 2020* (Eds: S. Tin, M. Hardy, J. Clews, J. Cormier, Q. Feng, J. Marcin, C. O'Brien, A. Suzuki), John Wiley & Sons, Inc. **2020**, 870.

[57] P. Caron, T. Khan, *Aerosp. Sci. Technol.* **1999**, *3*, 513.

[58] X.W. Jiang, D. Wang, G. Xie, H. Li, L.H. Lou, J. Zhang, *Metall. Mater. Trans. A*. **2014**, *45*, 6016.

[59] F. Lu, L.F. Li, S. Antonov, Y.F. Zheng, H.L. Fraser, D. Wang, J. Zhang, Q. Feng, in *Superalloys 2020* (Eds: S. Tin, M. Hardy, J. Clews, J. Cormier, Q. Feng, J. Marcin, C. O'Brien, A. Suzuki), John Wiley & Sons, Inc. **2020**, 218.

[60] Z. Fan, X. Wang, Y. Yang, H. Chen, Z. Yang, C. Zhang, *Mater. Sci. Eng. A.* **2019**, *748*, 267.

[61] S. Neumeier, H.U. Rehman, J. Neuner, C.H. Zenk, S. Michel, S. Schuwalow, J. Rogal, R. Drautz, M. Göken, *Acta Mater.* **2016**, *106*, 304.

[62] I. Lopez-Galilea, C. Zenk, S. Neumeier, S. Huth, W. Theisen, M. Göken, *Adv. Eng. Mater.* **2014**, *17*, 741.

[63] S. Giese, A. Bezold, M. Pröbstle, A. Heckl, S. Neumeier, M. Göken, *Metall. Mater. Trans. A.* **2020**, *51*, 6195.

[64] D.R. Goldstein, *J. Am. Stat. Assoc.* **2005**, *100*, 1464.

Accepted Article

15272648, 2023, 0, Downloaded from https://onlinelibrary.wiley.com. By MPI 337 Iron Research - on 02. Februar 2023. Re-use and distribution is strictly not permitted, except for Open Access articles

This article is protected by copyright. All rights reserved

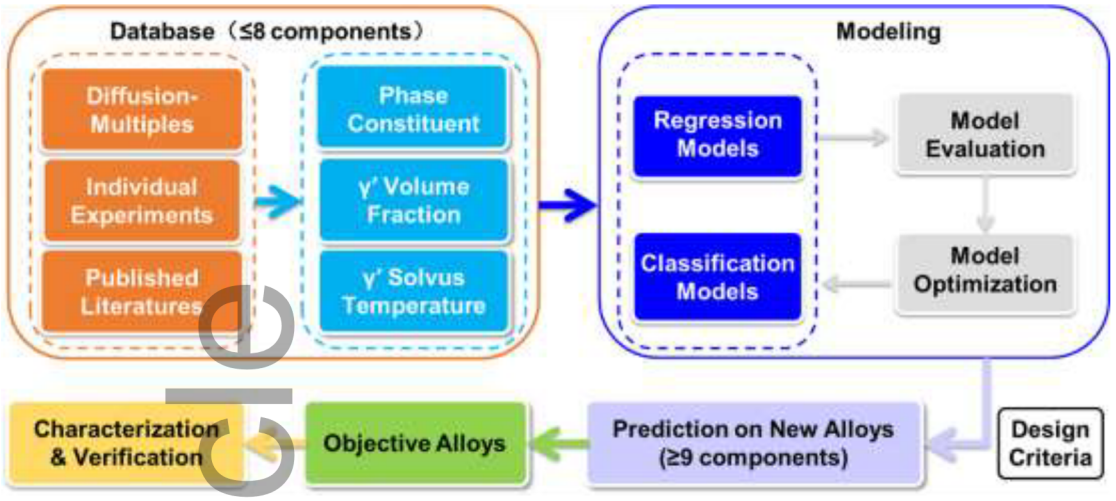


An integrated approach to designing the high-component (>7) γ′-strengthened Co-based superalloys with well-balanced properties is developed by combining the diffusion-multiples and machine-learning models. A "cross-component" prediction is achieved by the machine-learning models, where two types of novenary superalloys are screened out for aero-engine and industrial gas turbine blades, respectively, based on the experimental database mainly consisting of 6-7 elements.

Accepted Article

15272648, 2023, 0, Downloaded from https://onlinelibrary.wiley.com. By MPI 337 Iron Research - on 02. Februar 2023. Re-use and distribution is strictly not permitted, except for Open Access articles

This article is protected by copyright. All rights reserved